Supplementary Materials

Title: Comparing surface properties of melanoma cells using time of flight secondary ions mass spectroscopy

Authors: J. Bobrowska[a],†, J. Moffat[b],†, K. Awsiuk[c], J. Pabijan[a], J. Rysz[c], A. Budkowski[c], M. Reading[d], M. Lekka[a]*

[a] *The Institute of Nuclear Physics, Polish Academy of Sciences, Radzikowskiego 152, 31-342 Kraków, Poland,*

[b] *School of Pharmacy, University of East Anglia, Norwich, NR4 7TJ, United Kingdom,*

[c] *The Institute of Physics, Jagiellonian University, Lojasiewicza 11, 30-348 Kraków, Poland,*

[d] *School of Applied Sciences, University of Huddersfield, Queensgate, Huddersfield, HD1 3DH, United Kingdom.*

† J.B. and J.M. contributed equally to this work

* the corresponding author details:

Małgorzata Lekka

The Institute of Nuclear Physics PAS

Malgorzata.Lekka@ifj.edu.pl

Abstract

Various techniques have been already reported to differentiate between normal (non-malignant) and cancerous cells based on their physico-chemical properties. This is relatively easy when studied cancerous cells originate from distant stages of cancer progression. Here, studies on chemical properties of two closely related human melanoma cell lines are presented i.e. WM115 melanoma cells were taken from vertical growth phase while WM266-4 from skin metastatic site of the same patient. Their chemical properties were studies by two techniques, namely, time-of-flight secondary ion mass spectra (ToF SIMS) and photothermal microspectroscopy (PTMS), used to record mass and photothermal spectra of cells, respectively. In our approach, independently of the spectra type, its full range, i.e. masses and wavenumbers within the range 0–500 kDa and 500– 4000 cm-1, underwent a similar methodology for principal component analysis (PCA). The obtained results support the hypothesis that cancer-related alterations predominantly occurred at the cell surface and thus it is possibly to see PCA based data separation regardless of spectra type. Moreover, based on mass and photothermal spectra, fingerprints corresponding to phospholipids, in particular to phosphocholine, were responsible for the differentiation between melanoma cells, indicating

that the transition from vertical melanoma growth phase to metastasis induces changes in choline metabolism and phosphocholine accumulation in metastatic cells.

S1. PCA results for ToF SIMS mass spectra

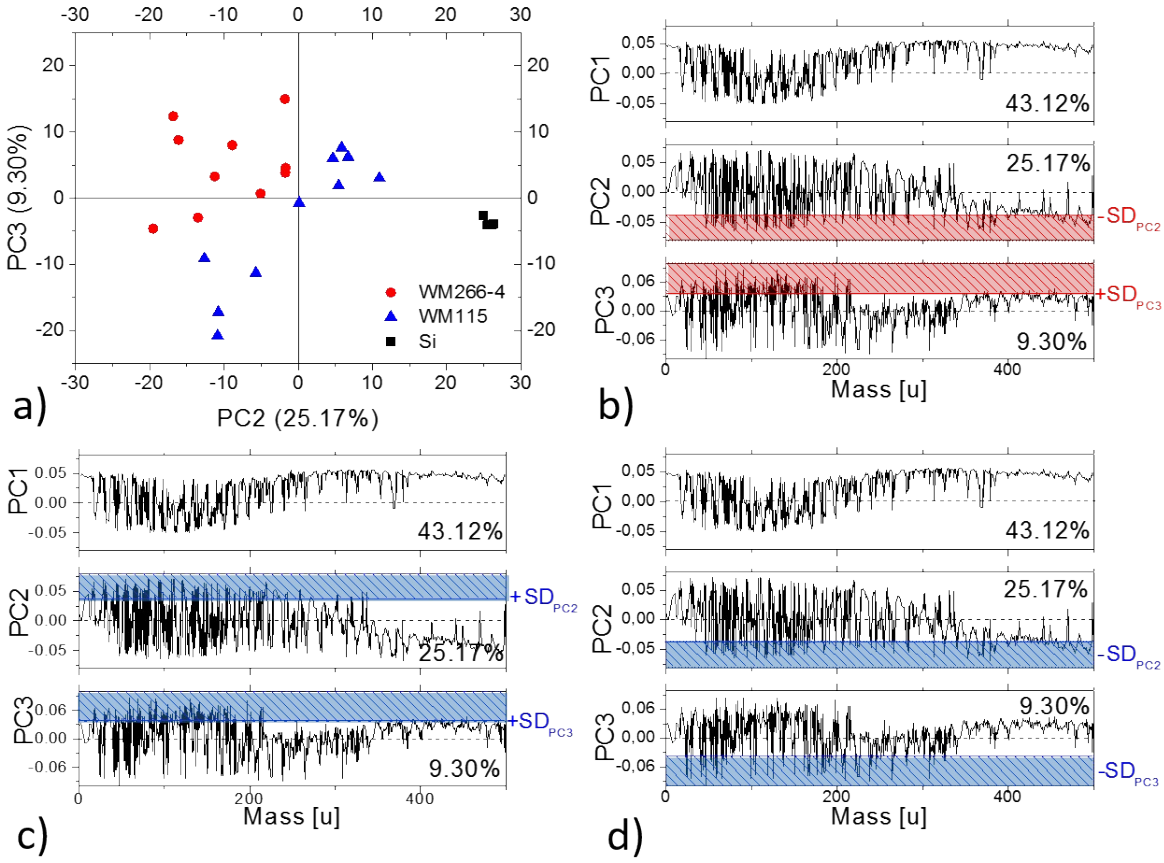

Figure S1. *(a) PC3 plotted as a function of PC2 showing data sets of (1) WM115 melanoma cells originating from vertical growth phase (blue triangles) and (2) WM266-4 cells originated from skin metastasis (red dots), and (3) the silicon surface used as reference (black squares); (b-d) Loadings plots obtained for each principal component PC1, PC2 and PC3, respectively, with marked threshold values (standard deviations). (b) Molecular masses below and above threshold values indicating masses that contributing strongly to separation of WM266-4 cells (marked in red). (c-d) Molecular masses below and above the corresponding threshold values indicating masses contributing strongly in separation of WM115 melanoma cells (marked in blue).*

Table S1. Summary of molecular masses that separates the studied melanoma cells, observed in the PC3–PC2 plot (Figure 2) found on the basis of analysis threshold values under conditions that:

(1) PC3 loading value > SDPC3 and PC2 loading value < -SDPC2 (WM266-4 data, results marked in red);

(2) PC3 loading value > SDPC3 and, simultaneously, PC2 loading value < -SDPC2 (WM115 cells, results marked in blue);

(3) PC3 loading value > SDPC3 and PC2 loading value > SDPC2 or PC3 loading value < -SDPC3 and PC2 loading value < -SDPC2 . (WM115 cells, results marked in blue).

Mass [u]	Chemical formula	Mass [u]	Chemical formula
16,02	NH_2^+	123,06	$C_6H_7N_2O^+$
17,03	NH_3^+	125,00	$Si_3C_3H_5N_2^+$
18,04	NH_4^+	126,09	$C_7H_{12}NO^+$
30,04	CH_4N^+	135,07	$C_5H_{11}O_4^+$
31,04	CH_5N^+	137,07	$C_2H_{11}SN_5^+$
32,05	CH_6N^+	142,94	$Na_2SO_4H^+$
40,02	$C_2H_2N^+$	146,06	$C_7H_6N_4^+$
44,01	$C_2H_6N^+$	150,08	$C_5H_{13}NPO_2^+$
46,03	CH_4NO^+	155,09	$C_{12}H_{11}^+$
52,02	CH_3NNa^+	155,15	$C_{10}H_{19}O^+$
53,04	$C_4H_5^+$	157,08	$C_{11}H_{19}O^+$
55,02	$C_3H_3O^+$	159,10	$C_{10}H_{11}N_2^+$
55,05	$C_4H_7^+$	164,92	$Na_3SO_4^+$
57,02	$SiC_2H_5^+$	166,08	$C_5H_{13}NPO_3^+$
57,05	$C_3H_7N^+$	168,08	$C_{12}H_{10}N^+$
57,07	$C_4H_9^+$	172,08	$C_{12}H_{12}O^+$
58,03	$C_2H_4NO^+$	173,10	$C_{12}H_{13}O^+$
58,06	$C_3H_8N^+$	174,10	$C_{12}H_{14}O^+$
59,07	$C_3H_9N^+$	184,10	$C_5H_{15}NPO_4^+$
60,08	$C_3H_{10}N^+$	185,10	$C_{13}H_{13}O^+$
61,01	$C_2H_5S^+$	186,09	$C_9H_{14}O_4^+$
65,04	$C_5H_5^+$	195,10	$C_{13}H_{11}N_2^+$
66,04	$C_5H_6^+$	198,10	$C_6H_{17}NPO_4^+$
67,04	$C_4H_5N^+$	199,11	$C_{14}H_{15}O^+$
67,05	$C_5H_7^+$	206,09	$C_5H_{14}NPO_4Na^+$
69,07	$C_4H_5O^+$	215,12	$C_{11}H_{19}O_4^+$
71,01	$C_3H_3O_2^+$	224,11	$C_8H_{19}NPO_4^+$
71,98	$CSN2^+$	225,12	$C_{12}H_{17}O_4^+$
77,00	C_5HO^+	226,11	$C_{12}H_{18}O_4^+$
87,95	$FeNOH_2$	240,13	$C_{19}H_{12}^+$
87,97	$SiN_2O_2^+$	246,11	$C_8H_{18}NPONa^+$
90,04	$C_3H_8SN^+$	255,13	$C_{13}H_{19}O_5^+$
98,02	$C_4H_4NO^+$	264,26	$C_{19}H_{36}^+$
98,98	C_3HSNO^+	281,10	$C_{12}H_{18}O_6Na^+$
102,09	$C_5H_{12}NO^+$	282,14	$C_{21}H_{30}^+$
104,11	$C_5H_{14}N^+$	313,27	$C_{19}H_{37}O_3^+$
107,05	$C_7H_7O^+$	410,21	$C_{19}H_{31}O_8Na^+$
108,94	$Si_3C_2H^+$	448,22	$C_{26}H_{49}O_3K^+$
120,08	$C_8H_{10}N^+$	454,22	$C_{21}H_{35}O_9Na^+$
122,06	$C_3H_8NO_2S^+$	474,23	$C_{29}H_{46}O_5^+$

S2. Results of PCA of SIMS spectra without Si reference spectra

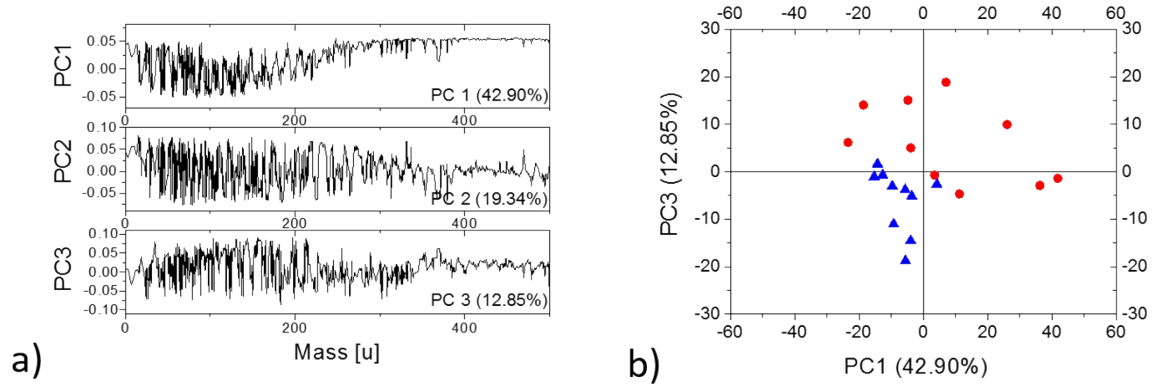

Figure S2. (a) Loading values for principal components PC1, PC2 and PC3, respectively, in relation to the original mass value. (b) PC3–PC2 plot with linear regression and 95% confidence bands fitted to the corresponding data sets (WM115 – blue triangles; WM266-4 – red dots).

S3. PCA results for PTMS spectra

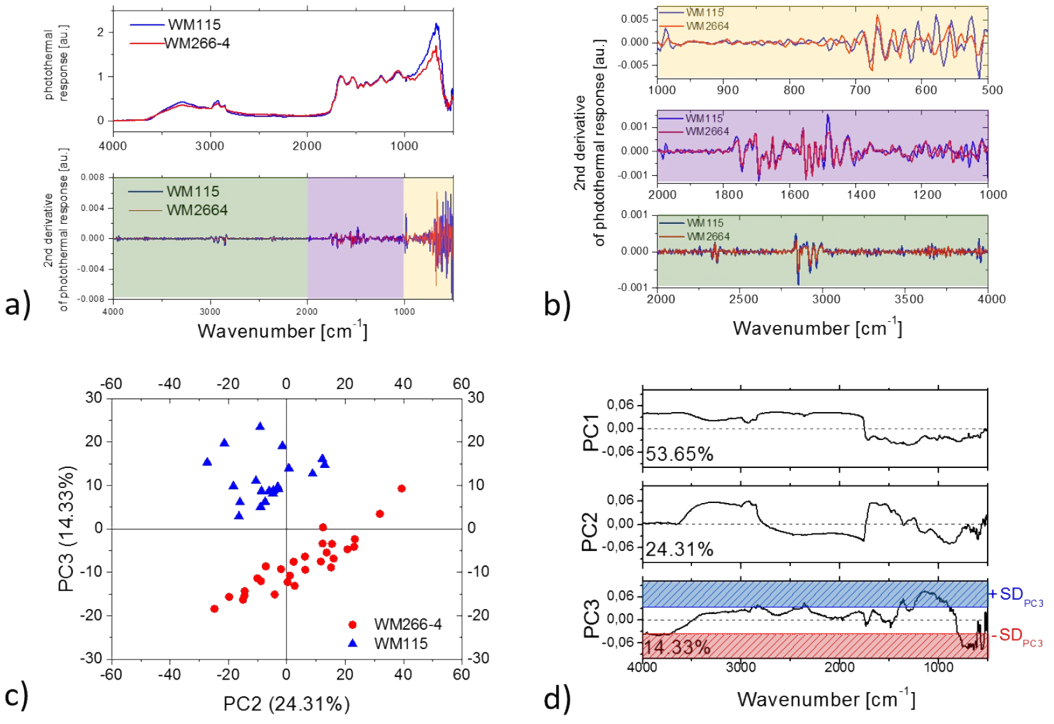

Figure S3. *(a) PC3 plotted as a function of PC2. (b) Loadings values for principal components PC1, PC2 and PC3, respectively, in relation to the wavenumber. Region with values of PC3 loadings higher than $+SD_{PC3}$ is marked in blue (corresponding to WM115 melanoma cells) and region with PC3 loadings lower than $–SD_{PC3}$ is marked in red (corresponding to WM266-4 metastatic melanoma cells).*

Table S2. Spectral ranges indicating molecules that contribute strongly to the data separation as observed in PC3-PC2 plot for melanoma cells, determined under condition that PC3 loading value < $-SD_{PC3}$ and PC3 loading value > SD_{PC3}.

Wavenumber region [cm^{-1}]	Examples of vibrational mode types present in the detected spectral range (molecule type; [ref])
4000-3700	broad O–H and N–H stretching
2780–2890	2874 cm^{-1} – symmetric C–H stretching vibrations of CH_3 (lipids; [1]) 2850 cm^{-1} – symmetric C–H stretching vibrations of CH_2 (lipids, choline, phospholipids; [2])
2300–2380	CH stretch combinations
1320–1410	1397 cm^{-1} – symmetric stretching of COO^- [1] 1379 cm^{-1} – symmetric bending of CH_3 (proteins, lipids; [1])
890–1260	1230 cm^{-1} - 1245 cm^{-1} – antisymmetric stretching of PO_2^- (DNA, RNA; [4], phospholipids, phosphorylated proteins; [1]) 1237 cm^{-1} – antisymmetric stretching of PO_2^- (phospholipids, proteins; [2]) 1173 cm^{-1} – antisymmetric stretching of –CO–O–C (esters; [1]) 1160 cm^{-1} - 1120 cm^{-1} – stretching of C–O (RNA ribose; [3]) 1150 cm^{-1} – C–O stretching, C–O–H bending (carbohydrates, mucin; [2]) 1083 cm^{-1} – symmetric stretching of PO_2^- (proteins, phospholipids, DNA; [2]) 1078 cm^{-1} – symmetric stretching of C–C (glycogen; [1]) 1063 cm^{-1} – symmetric stretching of –CO–O–C ([2] – phospholipids and cholesterol esters) 1050 cm^{-1}; 1060 cm^{-1}; 1015 cm^{-1} – symmetric stretching of C–O (carbohydrates, mucin; [2]; DNA, RNA ribose; [1]) 1050 cm^{-1} – stretching of C–O–P (phosphate ester; [1]) 1038 cm^{-1} – 1028 cm^{-1} – deflection C–H–O (glycogen; [1]) 968 cm^{-1} – stretching of C–O (DNA, phospholipids; 2]) 950 cm^{-1} – stretching of P–O (phosphorylated proteins; [1]) 920 cm^{-1} – stretching of C–O–P (phosphorylated proteins; [1])
610–805	'Fingerprint region' 730 cm^{-1}; 720 cm^{-1}; 718 cm^{-1} – CH_2 rocking (lipids, [3]) 725 cm^{-1}– bending of N–H bending (amide bands of proteins, [3]) 627 cm^{-1}– bending of O=C–N bending (amide bands of proteins, [3]) 600 cm^{-1} – bending of C=O (amide bands of proteins, [3])
530–570	'Fingerprint region'

1 G.Bellisola, C.Sorio, *Am. J., Cancer Res*. 2012 **2(1)** 1-21.
2 P. Lasch, M. Boese, A. Pacifico, M. Diem, *Vib. Spectrosc*., 2002, 28, 147–157.
3 B. Stuart, Biological Applications of Infrared Spectroscopy, *ACOL Series*, Wiley, Chichester, UK, 1997.
4 Benedetti, E., Bramanti, E., Papineschi, F., Rossi, I. and Benedetti E., *Appl. Spectrosc.,* 1997, **51**, 792–797.